IAI Journals.ASM.org

Relative Contributions of Lipooligosaccharide Inner and Outer Core Modifications to Nontypeable *Haemophilus influenzae* Pathogenesis

Pau Morey,[a,b] Cristina Viadas,[a,b,c] Begoña Euba,[b,c] Derek W. Hood,[d] Montserrat Barberán,[e] Carmen Gil,[c] María Jesús Grilló,[c] José Antonio Bengoechea,[a,b] Junkal Garmendia[a,b,c]

Laboratory Microbial Pathogenesis, Fundación Investigación Sanitaria Illes Balears (FISIB), CSIC-Govern de les Illes Balears, Bunyola, Spain[a]; Centro de Investigación Biomédica en Red de Enfermedades Respiratorias (CIBERES), Spain[b]; Instituto de Agrobiotecnología, CSIC-Universidad Pública Navarra-Gobierno Navarra, Mutilva, Spain[c]; Molecular Infectious Diseases Group, University of Oxford, Weatherall Institute of Molecular Medicine, John Radcliffe Hospital, Oxford, United Kingdom[d]; Facultad de Veterinaria, Universidad de Zaragoza, Zaragoza, Spain[e]

Nontypeable *Haemophilus influenzae* (NTHi) is a frequent commensal of the human nasopharynx that causes opportunistic infection in immunocompromised individuals. Existing evidence associates lipooligosaccharide (LOS) with disease, but the specific and relative contributions of NTHi LOS modifications to virulence properties of the bacterium have not been comprehensively addressed. Using NTHi strain 375, an isolate for which the detailed LOS structure has been determined, we compared systematically a set of isogenic mutant strains expressing sequentially truncated LOS. The relative contributions of 2-keto-3-deoxyoctulosonic acid, the triheptose inner core, oligosaccharide extensions on heptoses I and III, phosphorylcholine, digalactose, and sialic acid to NTHi resistance to antimicrobial peptides (AMP), self-aggregation, biofilm formation, cultured human respiratory epithelial infection, and murine pulmonary infection were assessed. We show that *opsX*, *lgtF*, *lpsA*, *lic1*, and *lic2A* contribute to bacterial resistance to AMP; *lic1* is related to NTHi self-aggregation; *lgtF*, *lic1*, and *siaB* are involved in biofilm growth; *opsX* and *lgtF* participate in epithelial infection; and *opsX*, *lgtF*, and *lpsA* contribute to lung infection. Depending on the phenotype, the involvement of these LOS modifications occurs at different extents, independently or having an additive effect in combination. We discuss the relative contribution of LOS epitopes to NTHi virulence and frame a range of pathogenic traits in the context of infection.

The Gram-negative opportunistic bacterial pathogen nontypeable (noncapsulated) *Haemophilus influenzae* (NTHi) is a common source of respiratory infection, is a primary causative agent of pediatric otitis media (OM), and is frequently isolated from adult patients suffering chronic respiratory diseases such as chronic obstructive pulmonary disease (COPD) (1). Lipopolysaccharide (LPS) is a major and essential component of the bacterial cell wall that has been associated with different aspects of *H. influenzae* pathogenicity (2–4). NTHi LPS contains no repetitive O-antigen side chains found in other Gram-negative bacteria and is referred to as lipooligosaccharide (LOS). NTHi LOS is a complex glycolipid comprising a membrane-anchoring lipid A linked by a single 2-keto-3-deoxyoctulosonic acid (Kdo) to a heterogeneous oligosaccharide composed mainly of neutral heptose (Hep) and hexose (Hex) sugars (5). Each Hep of a conserved trisaccharide inner core backbone can be a point for the addition of a Hex or further chain extensions, which constitute the outer core (for an example, see Fig. 1A). The genetic blueprint for NTHi LOS biosynthesis is known. Examples of genes involved in LOS biosynthesis that are relevant to this study include the following. *opsX* encodes a heptosyltransferase adding the first L-glycero-D-manno-heptose to Kdo (6). *lgtF*, *lic2C*, and *lpsA* each encode a glycosyltransferase responsible for adding a glucose (Glc) or a galactose (Gal) as the first sugar to Hep I, II, and III, respectively (7–9) (Fig. 1A). The *lic1* operon is responsible for the synthesis and transference of phosphorylcholine (PCho) (10). Finally, *lic2A* encodes a glycosyltransferase that adds a Gal as part of a digalactose epitope (11). The LOS of *Haemophilus* can also contain sialic acid (5-acetylneuraminic acid [Neu5Ac]) as a terminal sugar residue; *siaB* encodes a CMP-Neu5Ac synthetase which catalyzes the formation of CMP-Neu5Ac, a nucleotide sugar donor used by the sialyltransferases encoded by *lic3A*, *lic3B*, *siaA*, and *lsgB* (12–15).

The NTHi LOS molecule has been shown to participate in several aspects of NTHi-host interplay (3, 4). Current information on the role of LOS substitutions in NTHi infection is based on the loss of function for defined LOS truncations independently generated in nonisogenic genetic backgrounds. PCho can be a target for the acute-phase C-reactive protein (CRP), which triggers complement-mediated killing through the classical pathway (16–18), can correlate with increased outer membrane integrity and decreased binding of antibodies to LPS (19), and can contribute to NTHi resistance to the antimicrobial peptide (AMP) LL-37/hCAP18 (20). PCho also influences growth of NTHi as a biofilm (21–23), can facilitate bacterial interaction with the human respiratory epithelium (24), and can blunt the mouse pulmonary clearance of NTHi clinical isolates (25). The digalactose moiety confers resistance to killing by complement (17), and expression of two digalactosides may enhance *H. influenzae* virulence (26). Sialylated LOS glycoforms promote resistance to serum killing (14, 27) and play a role in formation of biofilms by NTHi (28–30). Despite the available evidence, there has not been any systematic phenotypic

Received 19 April 2013 Returned for modification 19 May 2013
Accepted 3 August 2013
Published ahead of print 26 August 2013
Editor: J. B. Bliska
Address correspondence to Junkal Garmendia, juncal.garmendia@unavarra.es.
P.M. and C.V. contributed equally to this article.
Supplemental material for this article may be found at http://dx.doi.org/10.1128/IAI.00492-13.

doi:10.1128/IAI.00492-13

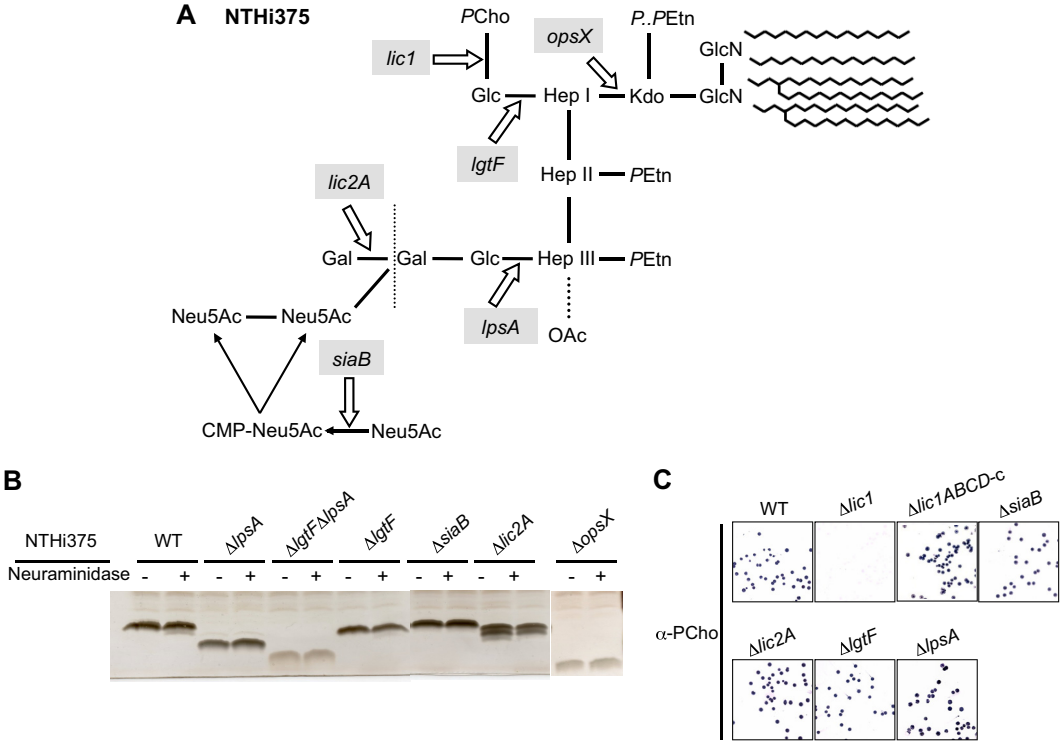

FIG 1 (A) LOS structure proposed for NTHi 375. Genes of interest, disrupted in this work, are indicated in gray, with white empty arrows indicating their point of action. (B) Electrophoretic profiles following SDS-PAGE of LOS isolated from the NTHi 375 wild type and Δ*lpsA*, Δ*lgtF*Δ*lpsA*, Δ*lgtF*, Δ*siaB*, Δ*lic2A*, and Δ*opsX* mutants. A pair of profiles, before (−) and after (+) neuraminidase treatment, is shown for each strain. (C) Detection of PCho epitope by colony immunoblotting on wild-type NTHi 375 (WT) and Δ*lic1*, Δ*lic1ABCD*-c, Δ*siaB*, Δ*lic2A*, Δ*lgtF*, and Δ*lpsA* mutants. GlcN, glucosamine; *P*Etn, phosphoethanolamine; Hep, heptose; Glc, glucose; Gal, galactose; *P*Cho, phosphorylcholine; OAc, O-acetyl; *P*, phosphate.

study on panels of isogenic mutants generated on a pathogenic strain to further our understanding of the specific and the relative roles of particular LOS structures in NTHi virulence. Based on this notion, we took advantage of NTHi strain 375 (hereafter referred to as NTHi 375), an isolate for which the detailed LOS structure has been determined (14, 31), to generate mutants defective for a range of LOS-specific enzymes, evaluate the effect of sequential LOS truncation on a range of virulence phenotypes, and assign specific roles in pathogenic properties to distinct moieties of the LOS. We considered the roles of Kdo, the triheptose inner core, oligosaccharide extensions on Hep I and III, PCho, digalactose, and sialic acid. We evaluated bacterial resistance to AMPs, self-aggregation and biofilm formation, infection of human respiratory epithelial cells (including bacterial adhesion, invasion, and cell inflammatory response), and persistence and clearance in a murine pulmonary model. This work provides a context for the relative importance of NTHi LOS moieties to a range of virulence traits, providing a greater understanding of LOS contribution to NTHi pathogenesis.

MATERIALS AND METHODS

Bacterial strains, media, and growth conditions. Strains used in this study are described in Table 1. NTHi strains were grown (overnight at 37°C and 5% CO_2) on chocolate agar plates (bioMérieux) or on brain heart infusion (BHI) agar plates supplemented with 10 μg/ml of hemin and 10 μg/ml of NAD, referred to as sBHI, and also with erythromycin at 10 μg/ml (Erm_{10}) or kanamycin at 11 μg/ml (Km_{11}), when required. *Escherichia coli* was grown on Luria-Bertani (LB) broth or LB agar plates at 37°C, supplemented with either ampicillin at 100 μg/ml (Amp_{100}) or erythromycin at 150 μg/ml (Erm_{150}), when necessary.

NTHi 375 is an OM isolate (14, 31); NTHi 375 Δ*lic1* has been described previously (32). Genes *hap* (NTHi0354), *siaB* (HI1279), *siaT* (HI0147), *lic2A* (HI550), *lgtF* (HI653), *lpsA* (HI765), and *opsX* (HI261), and their respective adjacent regions, were amplified by PCR with *Taq* polymerase (Promega) using NTH i375 genomic DNA as the template and primers hap-F1/hap-R1, siaB-F1/siaB-R1, siaT-F1/siaT-R1, lic2A-F1/lic2A-R1, lgtF-F1/lgtF-R1, lpsA-F1/lpsA-R1, and opsX-F1/opsX-R1, respectively. Primers were designed based on the genome sequences of *H. influenzae* strains Rd KW20 and NTHi 86-028NP (33, 34) (see Table S1 in the supplemental material). The gene-containing fragments were separately cloned into pGEM-T Easy (Promega), generating pGEMT/hap, pGEMT/siaB, pGEMT/siaT, pGEMT/lic2A, pGEMT/lgtF, pGEMT/lpsA, and pGEMT/opsX. Cloned PCR products were disrupted by inverse PCR with *Vent* polymerase (New England BioLabs), using primers hap-F2/hap-R2, siaB-F2/siaB-R2, siaT-F2/siaT-R2, lic2A-F2/lic2A-R2, lgtF-F2/lgtF-R2, lpsA-F2/lpsA-R2, and opsX-F2/opsX-R2, respectively (see Table S1). In all cases, an internal ~30-bp fragment was replaced by a blunt-ended (excised by SmaI) erythromycin resistance cassette from pBSLerm (35), generating plasmids pALG-1, pPMO-7, pSM-1, pPMO-8, pPMO-9, pPMO-10, and pPMO-11 (Table 1). These plasmids were digested with NotI to obtain linear disruption cassettes for *hap*, *siaB*, *siaT*, *lic2A*, *lgtF*, *lpsA*, and *opsX* that were used to transform NTHi 375 using the MIV method (36). Transformants were screened by plating bacteria on sBHI agar plates containing Erm_{10}. The NTHi 375 Δ*lgtF* Δ*lpsA* mutant was generated by two successive recombination events. First, strain NTHi 375 Δ*lgtF* was generated as described above, and then it was transformed with a disruption cassette for *lpsA*. This disruption cassette was generated by cloning a blunt-ended kanamycin resistance cassette released from

TABLE 1 Strains and plasmids used in this study

Strain or plasmid	Description	Reference or source
H. influenzae		
375	Wild type	31
375 Δ*lic1*	*lic1BC*::*ermC* Erm^r	32
375 Δ*siaB*	*siaB*::*ermC* Erm^r	This study
375 Δ*lic2A*	*lic2A*::*ermC* Erm^r	This study
375 Δ*lgtF*	*lgtF*::*ermC* Erm^r	This study
375 Δ*lpsA*	*lpsA*::*ermC* Erm^r	This study
375 Δ*lgtF* Δ*lpsA*	*lgtF*::*ermC lpsA*::*km* Erm^r Km^r	This study
375 Δ*opsX*	*opsX*::*ermC* Erm^r	This study
375 Δ*lic1ABCD*-c	*lic1BC*::*ermC Hi0601.1*::*km*::*lic1ABCD* Erm^r Km^r	This study
375 Δ*lic2A*-c	*lic2A*::*ermC Hi0601.1*::*km*::*lic2A* Erm^r Km^r	This study
375 Δ*lgtF*-c	*lgtF*::*ermC Hi0601.1*::*km*::*lgtF* Erm^r Km^r	This study
375 Δ*siaT*	*siaT*::*ermC* Erm^r	This study
375 Δ*hap*	*hap*::*ermC* Erm^r	This study
E. coli		
CC118	Used for cloning and aggregation assays	
Plasmids		
pGEM-T Easy	Used for cloning assays	Promega
pGEM-T/HI0601.1	Pseudogene HI0601.1 and flanking regions cloned into pGEM-T Easy	This study
pPMO-4	Derivative of pGEM-T/HI0601.1 Disruption of HI0601.1 from NTHi375 with a Km^r cassette	This study
pGEM-T/*siaB*	*siaB* from NTHi 375 and flanking regions cloned into pGEM-T Easy	This study
pGEM-T/*lic2A*	*lic2A* from NTHi 375 and flanking regions cloned into pGEM-T Easy	This study
pGEM-T/*lgtF*	*lgtF* from NTHi 375 and flanking regions cloned into pGEM-T Easy	This study
pGEM-T/*lpsA*	*lpsA* from NTHi 375 and flanking regions cloned into pGEM-T Easy	This study
pGEM-T/*opsX*	*opsX* from NTHi 375 and flanking regions cloned into pGEM-T Easy	This study
pGEM-T/*siaT*	*siaT* from NTHi 375 and flanking regions cloned into pGEM-T Easy	This study
pGEM-T/*hap*	*hap* from NTHi 375 (nucleotides 2028–4230) cloned into pGEM-T Easy	This study
pBSLerm	Source of an Erm^r cassette	35
pUC4K	Source of a Km^r cassette	Addgene
pPMO-7	pGEM-T/*siaB* derivative where *siaB* is disrupted by an Erm^r cassette	This study
pPMO-8	pGEM-T/*lic2A* derivative where *lic2A* is disrupted by an Erm^r cassette	This study
pPMO-9	pGEM-T/*lgtF* derivative where *lgtF* is disrupted by an Erm^r cassette	This study
pPMO-10	pGEM-T/*lpsA* derivative where *lpsA* is disrupted by an Erm^r cassette	This study
pPMO-11	pGEM-T/*opsX* derivative where *opsX* is disrupted by an Erm^r cassette	This study
pPMO-12	pGEM-T/*lpsA* derivative where *lpsA* is disrupted by a Km^r cassette	This study
pPMO-13	pMO-4 derivative where *Pr*::*lgtF* is cloned into pPMO-4, generating a disruption of HI0601.1	This study
pPMO-14	pPMO-4 derivative where *Pr*::*lic2A* is cloned into pMO-4, generating a disruption of HI0601.1	This study
pPMO-15	pPMO-4 derivative where *Pr*::*lic1ABCD* is cloned into pMO-4, generating a disruption of HI0601.1	This study
pSM-1	pGEM-T/*siaT* derivative where *siaT* is disrupted by an Erm^r cassette	This study
pALG-1	pGEM-T/*hap* derivative where *hap* is disrupted by an Erm^r cassette	This study

pUC4K by digestion with HincII in a vector obtained by inverse PCR of pGEM-T/*lpsA* with primers lpsA-F2/lpsA-R2. The resulting plasmid, pPMO-12, was digested with NotI, creating a 3.8-kb linear fragment which contains the disruption cassette *lpsA*::Km^r, used to transform NTHi 375 Δ*lgtF*. Double-recombination events were selected on sBHi agar containing Erm_{10} and Km_{11}.

Complementation of NTHi 375 Δ*lgtF*, Δ*lic2A*, and Δ*lic1* strains was carried out by inserting the relevant gene into open reading frame (ORF) HI0601.1; this ORF contains a frameshift in *H. influenzae* Rd KW20 (37). Copies of *lgtF*, *lic2A*, and *lic1ABCD* genes were used to complement the NTHi 375 Δ*lgtF*, Δ*lic2A*, and Δ*lic1* mutants, respectively. PCR was used to amplify a 2.3-kb fragment from NTHi 375 genomic DNA using primers HI0601.1-F1/HI0601.1-R1. This fragment was cloned into pGEM-T Easy and sequenced, confirming that HI0601.1 in NTHi 375 also contained a frameshift. HI0601.1 was disrupted by inverse PCR with *Vent* polymerase using primers HI0601.1-F2/HI0601.1-R2. An internal ~30-bp fragment was replaced by a kanamycin resistance cassette from pUC4K, generating pPMO-4. Genes *lgtF*, *lic2A*, and *lic1ABCD*, with their respective promoter regions, were amplified with *Vent* polymerase from NTHi 375 genomic DNA using primers lgtF-prF1/lgtF-stopR1, lic2A-prF1/lic2A-stop, and lic1-prF1/lic1-stopR1, respectively. These fragments were phosphorylated and ligated into a vector generated by inverse PCR of pPMO-4 with primers HI0601.1-R2/pUC4K-R1, creating pPMO-13, pPMO-14, and pPMO-15, respectively (Table 1). These plasmids were digested with NotI, generating DNA fragments of 3.9, 4.5, and 7.1 kb, used to transform NTHi 375 Δ*lgtF*, Δ*lic2A*, and Δ*lic1* strains, respectively. Complemented strains were selected on sBHi agar containing Erm_{10} and Km_{11}.

Preparation and neuraminidase treatment of LPS. Bacterial lysates were prepared from cells grown overnight on BHI plates supplemented with Levinthal's reagent (10%) and neuraminic acid (Neu5Ac; Boehringer Ingelheim) (50 μg/ml) and adjusted in phosphate-buffered saline (PBS) to an optical density at 260 nm (OD_{260}) of 1. Ten-microliter suspensions were lysed by boiling for 5 min. The lysates were treated (37°C overnight) with 2.5 μl of neuraminidase (4 U/μl) from *Clostridium perfringens* (Boehringer Ingelheim) and subsequently boiled for 5 min.

LPS electrophoretic separation. The patterns of LPS isolated from wild-type and mutant strains of *H. influenzae*, before and after neuraminidase treatment, were determined after fractionation by tricine-SDS-polyacrylamide gel electrophoresis (T-SDS-PAGE) (38) using 17.7% gels and silver staining (Quicksilver; Amersham, United Kingdom) according to the manufacturer's instructions. Gels were scanned and images were recorded for densitometry analysis using ImageJ software; bands in each lane were analyzed, and lane profile plots were generated.

Colony immunoblotting. An assessment of PCho levels on the surface of NTHi strains was carried out by colony immunoblotting using TEPC-15 antibody (Sigma), as previously described (39).

Antimicrobial peptide susceptibility assay. The antimicrobial peptide susceptibility assay was adapted from reference 40. Bacteria were grown on 10 ml of sBHI to the exponential growth phase ($OD_{650} = 0.3$) and then harvested by centrifugation at 3,500 × *g* for 20 min at 20°C. Bacteria were washed once with PBS, and a suspension containing ~10^5 CFU/ml was prepared in 10 mM PBS (pH 6.5), 1% tryptone soy broth (TSB; Oxoid), and 100 mM NaCl. Aliquots of 5 μl of this suspension were mixed in microcentrifuge tubes with various concentrations of polymyxin B (PxB) or human β defensin-1 (hBD-1) (prepared in 10 mM PBS [pH 6.5], 1% TSB, and 100 mM NaCl). In all cases, the final volume was 30 μl. After 60 min of incubation at 37°C, surviving bacteria were enumerated following culture on sBHI agar. Results are expressed as the ratio of the number of bacteria surviving compared to the number of bacteria in a control lacking antimicrobial peptide (AMP), expressed as a percentage. The 50% inhibitory concentration (IC_{50}) of PxB was defined as the concentration producing a 50% reduction in the colony counts compared to those of bacteria not exposed to the antibacterial agent. According to guidelines of the NIH Chemical Genomics Center, the IC_{50} of a given drug was determined from a dose-response curve data fit using a standard four-parameter logistic nonlinear regression analysis. Dose-response experiments were performed in duplicate, on at least four independent occasions ($n \geq 8$).

Bacterial aggregation assay. Three or four colonies of NTHi or *E. coli* grown on chocolate agar or LB plates, respectively, were inoculated into 20 ml of sBHI (NTHi) or LB (*E. coli*) medium, grown overnight, diluted in the same medium to an OD_{600} of 1, and left standing at room temperature for 7 h (starting volume, ~20 ml). The viability of each culture was tested by serial dilution and plating on sBHI agar or LB agar. OD_{600} readings were performed at regular intervals on 500-μl aliquots collected from the top of each bacterial suspension. At least four independent experiments ($n \geq 4$) were performed for each strain.

Biofilm formation. Biofilm formation under flow conditions was assessed using 60-ml microfermentors (Pasteur Institute, Laboratory of Fermentation) with a continuous flow of medium (40 ml/h) and constant aeration with sterile compressed air (30,000 Pa). Submerged Pyrex glass slides served as the growth substratum. Three or four colonies of each strain grown on chocolate agar plates were inoculated in 20 ml of sBHI medium and incubated with shaking up to an OD_{600} of 1. Approximately 10^8 bacteria from this culture were used to inoculate the microfermentor, which was then run at 37°C for 16 h. The viability of each inoculated bacterial aliquot was tested by serial dilution and plating on sBHI agar. Biofilm development was recorded with a Nikon Coolpix 950 digital camera. To quantify the biofilm formed, bacteria adhered to the Pyrex slides were resuspended in 10 ml of PBS. The OD_{600} of the suspensions was determined. Experiments were performed on at least three independent occasions ($n \geq 3$).

Epithelial cell culture and bacterial infection. Carcinomic human alveolar basal epithelial cells (A549, ATCC CCL-185) were maintained as described before (41). Cells were seeded at 6×10^4 cells/well in 24-well tissue culture plates for 32 h and serum starved 16 h before infection, reaching 90% cellular confluence at the time of infection. For NTHi infection, bacteria were recovered with 1 ml of PBS from a chocolate agar plate grown for 16 h. The bacterial suspension was adjusted to an OD_{600} of 1 in PBS (~10^9 CFU/ml). A549 cells were infected in 1 ml of Earle's balanced salt solution (EBSS; Gibco) to get a multiplicity of infection of ~100:1. For adhesion experiments, cells were infected for 30 min, washed 5 times with PBS, and lysed with 300 μl of PBS-saponin (0.025%) for 10 min at room temperature, and serial dilutions were plated on sBHI agar. For invasion assays, cells were infected for 2 h, washed 3 times with PBS, and incubated for 1 h with RPMI 1640 containing 10% fetal calf serum (FCS), HEPES, and gentamicin (200 μg/ml) to kill extracellular bacteria. Cells were washed 3 times with PBS and lysed as described before. In all cases, infection experiments were carried out in triplicate and on at least three independent occasions ($n \geq 9$).

Secretion of IL-8. A549 cells were maintained and infected for 2 h, as described above. Cells were washed 3 times with PBS and incubated with fresh medium containing gentamicin (100 μg/ml) for 6 or 20 h. Supernatants were removed from the wells, cell debris was removed by centrifugation, and samples were frozen at −80°C. Interleukin 8 (IL-8) levels in the supernatants were measured using an enzyme-linked immunosorbent assay (ELISA) kit (Innova). Infection experiments were carried out in duplicate and on at least two independent occasions ($n \geq 4$).

Mouse assays. CD1 female mice (4 to 5 weeks old) were purchased from Charles River Laboratories and housed under pathogen-free conditions at the Institute of Agrobiotechnology facilities (registration number ES/31-2016-000002-CR-SU-US). For NTHi infection, bacteria were recovered with 1 ml of PBS from a chocolate agar plate grown for 16 h, to obtain a suspension of ~5×10^9 CFU/ml. Before infection, mice were anesthetized by intraperitoneal inoculation of a mixture of ketamine-xylazine (3:1). Each mouse received 20 μl of inoculum (~10^8 CFU) intranasally. Groups of 5 mice were euthanized and necropsied at selected intervals, to obtain samples from upper airways, tracheas, and lungs for histopathological studies and/or to determine the number of CFU per lung.

Histopathology and lesion score. Heads, tracheas, and lower respiratory tracts with lungs from mice infected with NTHi 375 were aseptically removed, at 24 and 48 h postinfection (p.i.), during necropsy. Animals receiving 20 μl of PBS intranasally were used as controls. Heads were immersed in 10% neutral buffered formalin and maintained for 2 days, rinsed in running tap water for 2 h, and decalcified with 5% nitric acid for 24 to 36 h. After complete fixation and decalcification, 5 transaxial slices were made every 3 to 4 mm beginning at the nostrils and finishing in the nasopharynx. Tracheas and lungs were fixed overnight in 10% buffered formalin and embedded in paraffin, and 4- to 6-μm sections were stained with hematoxylin and eosin (H&E) by standard procedures and examined by microscopy to determine the presence and extent of inflammation and lesions. Lesions in the airways and lungs were subjectively scored on a scale of 0 to 3 (0, absent; 1, mild; 2, moderate; and 3, severe) depending on the percentage of tissue affected, the epithelial changes, the degree of inflammatory cell infiltration, and the degree and type of exudates in lumens. Similar sections were stained for immunohistochemistry (IHC). Sections were subjected to antigen retrieval by heating the slides in a pressure cooker for 3 min in distilled water pH 4.0. IHC staining was performed using an EnVision horseradish peroxidase (HRP) kit (Dako Corporation, USA) and a polyclonal rabbit anti-NTHi antibody (41). For tissue controls, similar organs obtained from noninfected mice were processed in a manner identical to that for the infected tissues. For a serum control, similar sections of tissues obtained from infected mice were processed using a conventional rabbit serum. The images were observed and digitalized using an Olympus Vanox AHBS3 microscope coupled to an Olympus DP12 digital camera.

Lung bacterial counting. Mice ($n = 5$) were infected intranasally with wild-type or mutant strains. Lungs were aseptically removed, individually weighed in sterile bags (Stomacher 80; Seward Medical), homogenized, and serially 10-fold diluted in PBS. Each dilution was spread on sBHI agar plates to determine the number of viable bacteria (detection limit < 10 CFU/lung). The individual number of CFU/lung was logarithmically transformed for data normalization and graphically represented by box plot using the StatViewGraphics 5.0 for Windows (SAS Institute Inc.)

TABLE 2 NTHi LOS sequential mutant strains resistance to polymyxin B- and human β-defensin 1 (μg/ml)-mediated killing after bacterial incubation with the AMP

Strain name or genotype	% survival[a] at indicated concn(μg/ml) of:					
	Polymyxin B					
	1	0.75	0.5	0.25	0.125	hBD-1, 0.5
NTHi 375	5.6 ± 4	13.7 ± 8.5	92.1 ± 11.4	99.7 ± 9.7	101.1 ± 10.9	90.3 ± 8.4
Δ*lic1*	2.2 ± 1	11.9 ± 3.6	30.9 ± 4.7[b]	91.3 ± 4.9	92.1 ± 2.9	52.6 ± 19.1[b]
Δ*lic1ABCD*-c	5.9 ± 2.8	13.9 ± 6.6	87.5 ± 15.9	102.5 ± 20.1	97.4 ± 4.8	87.5 ± 14.6
Δ*siaB*	5.7 ± 8	14.2 ± 19.7	98.1 ± 11.7	121.1 ± 10.4	111.8 ± 12.5	85.2 ± 10.5
Δ*lic2A*	1.9 ± 2.4[b]	4.8 ± 2.5[b]	69.6 ± 4.1[b]	93 ± 5.2	102.1 ± 5	74 ± 8.3[b]
Δ*lic2A*-c	5.2 ± 3.5	8.6 ± 4.3	93.9 ± 2.8	108.4 ± 4	100 ± 3.2	102.1 ± 9.4
Δ*lgtF*	3.5 ± 5.5	8.7 ± 7.5	53.5 ± 9.3[b]	67.7 ± 8[b]	95.8 ± 7.4	57.2 ± 7.4[b]
Δ*lgtF*-c	6.1 ± 4.2	9.9 ± 3.3	96 ± 5.4	101.3 ± 5.2	107.8 ± 6	101.2 ± 2.8
Δ*lpsA*	1.3 ± 1.5[b]	2.8 ± 2.5[b]	72.6 ± 8.2[b]	92.1 ± 6.5	97.1 ± 11.7	78.5 ± 5.5[b]
Δ*lgtF* Δ*lpsA*	0[b]	0.1 ± 0.1[b]	24.6 ± 4.5[b]	78.2 ± 6.2[b]	92.7 ± 1.8	35.4 ± 7[b]
Δ*opsX*	0[b]	0[b]	3.2 ± 3.8[b]	9.5 ± 10[b]	13.4 ± 7.3[b]	28.9 ± 10.9[b]

[a] Expressed as percentage of survival of untreated bacteria (considered as 100%).
[b] $P < 0.05$ versus parental NTHi 375 tested at each given concentration.

statistical package. Box whiskers represent 99% of data; lines inside boxes represent median values.

Statistical analysis. For AMP resistance, self-aggregation, biofilm growth, epithelial cell infection, and IL-8 secretion assays, means ± standard deviations (SDs) were calculated, and statistical comparison of means were performed using the two-tailed *t* test. In mouse experiments, statistical comparisons of mean $\log_{10}$ CFU/lung were performed by a one-way analysis of variance (ANOVA) followed by the Fisher's protected least significant difference (PLSD) tests. In all cases, a *P* value of <0.05 was considered statistically significant. Analyses were performed using the Prisma4 for PC (GraphPad Software) or StatViewGraphics 5.0 for Windows (SAS Institute Inc.) statistical package.

RESULTS

Construction and characterization of sequential LOS truncations on NTHi 375. We constructed a set of mutant strains expressing sequentially truncated LOS molecules in NTHi 375; this isolate has been used for previous studies on NTHi biology and infection (14, 32, 41), and its LOS structure has been determined (Fig. 1A). We generated NTHi 375 Δ*siaB*, Δ*lic2A*, Δ*lgtF*, Δ*lpsA*, Δ*lgtF* Δ*lpsA*, and Δ*opsX* mutant strains. Table 1 lists all strains used in this work. The profiles of LOS purified from wild-type and mutant strains were analyzed by tricine-SDS-PAGE and staining with silver, following neuraminidase treatment to assess the presence of sialic acid. LOS from NTHi 375 Δ*lgtF*, Δ*lic2A*, Δ*lpsA*, Δ*lgtF* Δ*lpsA*, and Δ*opsX* mutants showed a stepwise decrease in molecular weight (Fig. 1B; see also Fig. S1A in the supplemental material). Neuraminidase treatment resulted in the appearance of a lower band in the LOS profile from the wild-type and Δ*lgtF* strains, corresponding to a loss of Neu5Ac from sialylated glycoforms, and in removal of the lowest band in LOS from the Δ*lic2A* mutant strain (Fig. 1B; see also Fig. S1B). The presence of PCho was assessed on the panel of mutant strains by colony immunoblotting using mouse anti-PCho antibody TEPC-15. Wild-type, Δ*siaB*, Δ*lic2A*, Δ*lgtF*, and Δ*lpsA* strains showed reactivity to TEPC-15, while the Δ*lic1* (32, 41), Δ*lgtF* Δ*lpsA*, and Δ*opsX* strains did not (Fig. 1C and data not shown). Complementation of the *lic1* mutation (NTHi 375 Δ*lic1ABCD*-c strain) restored a PCho signal comparable to that observed with the wild-type strain (Fig. 1C). The NTHi 375 Δ*lgtF* mutant displayed a PCho signal similar to that of the wild-type strain, suggesting that on NTHi 375, some PCho could be linked to the Glc attached to Hep III in the absence of the Glc added by LgtF. None of the mutants exhibited growth defects compared to the wild-type when grown in liquid culture (data not shown).

LOS truncation increases susceptibility to soluble elements of innate immunity. Antimicrobial peptides (AMPs) play an important role in host protection against infections, and pathogens have developed strategies to counteract their antimicrobial action (42–45). We evaluated the contribution of LOS moieties on NTHi 375 to resistance to AMP-mediated killing. First, we studied the survival of the wild-type and mutant strains in the presence of increasing doses of PxB. PxB is an experimental substitute for AMPs, commonly used to demonstrate AMP resistance in laboratory settings because of a similar mechanism of action against Gram-negative bacteria (46, 47). The results are shown in Table 2 and in Fig. S2 in the supplemental material. NTHi 375 Δ*lic1* was more susceptible to PxB than the wild-type strain, supporting previous observations with different AMPs (20). The Δ*lic1*ABCD-c complemented strain restored this deficiency. NTHi 375 Δ*siaB* showed no significant change in resistance to PxB compared to the wild-type strain. This observation was supported by NTHi 375 Δ*siaT*, a mutant strain deficient in sialic acid uptake. The Δ*lic2A* and Δ*lpsA* mutants showed a slight increase in susceptibility to PxB, which may be due to the absence of digalactose in each case. Resistance was restored to a wild-type level in the Δ*lic2A*-c complemented strain. NTHi 375 Δ*lgtF* displayed lower resistance to PxB than did the wild-type strain, suggesting that the addition of Glc on Hep I or its substitution with PCho contribute to bacterial resistance to AMPs. Strains NTHi 375 Δ*lgtF* Δ*lpsA* and Δ*opsX* were the most susceptible ones, suggesting a correlation between increasing LOS truncation and higher sensitivity. Data obtained for NTHi 375 Δ*lgtF* Δ*lpsA*, compared to those of Δ*lgtF* and Δ*lpsA* mutants, suggest that the two LOS substitutions play nonredundant roles on NTHi resistance to PxB.

Similar findings were obtained when the susceptibility of the strains to hBD-1, a natural AMP found in the airway (48), was assessed (Table 2).

Together, these results suggest contributions for the triheptose inner core, sugar extensions on Hep I and III, PCho, and digalac-

TABLE 3 Self-aggregation (decrease of absorbance at 600 nm) of NTHi mutant strains expressing truncated LOS with time

Strain name or genotype	Decrease of absorbance at 600 nm at:						
	1 h	1.5 h	2 h	3 h	4 h	5 h	6 h
E. coli CC118	1.03	1.03	1.04	1.03	1.04	1.03	1.03
NTHi 375	0.98 ± 0.1	0.71 ± 0.1	0.53 ± 0.1	0.28 ± 0.1	0.17 ± 0.1	0.11	0.08
Δ*hap*	1.03 ± 0.02	0.95 ± 0.03	0.84 ± 0.06	0.69 ± 0.1	0.56 ± 0.06	0.47 ± 0.04	0.36 ± 0.06
Δ*lic1*	0.58 ± 0.1[a]	0.36 ± 0.1[a]	0.22[a]	0.07[a]	0.05[a]	0.03[a]	0.02[a]
Δ*lic1ABCD*-c	0.91 ± 0.1	0.69 ± 0.2	0.5 ± 0.2	0.22 ± 0.1	0.14 ± 0.1	0.08	0.06
Δ*siaB*	1.04 ± 0.1	0.78 ± 0.1	0.6 ± 0.2	0.29 ± 0.1	0.18 ± 0.1	0.12 ± 0.1	0.08
Δ*lic2A*	0.99 ± 0.1	0.68 ± 0.2	0.44 ± 0.2	0.19 ± 0.1	0.1	0.08	0.06
Δ*lgtF*	0.96 ± 0.1	0.75 ± 0.2	0.58 ± 0.2	0.32 ± 0.2	0.21 ± 0.1	0.16 ± 0.1	0.11
Δ*lpsA*	0.92 ± 0.2	0.6	0.35	0.18	0.1	0.06	0.05
Δ*lgtF* Δ*lpsA*	0.99 ± 0.1	0.64 ± 0.1	0.34 ± 0.1	0.15	0.08	0.07	0.04
Δ*opsX*	1.01	0.85 ± 0.1	0.61 ± 0.1	0.28 ± 0.1	0.17	0.12	0.08

[a] OD_{600} values for NTHi 375 Δ*lic1* were significantly lower ($P < 0.0001$ at 1 to 1.5 h; $P < 0.05$ from 2 h to the end of the assay) than those obtained for the wild-type strain.

tose to NTHi resistance to AMP-mediated killing. A correlation between serial LOS truncation and AMP sensitivity could be established for PxB and hBD-1.

Heterogeneous effect of LOS truncation on self-aggregation and biofilm formation. NTHi undergoes self-aggregation, which may promote microcolony formation on host cell surfaces (49). To investigate the contribution of LOS structure to NTHi forming aggregates, we performed tube-settling assays with the panel of NTHi 375 mutant strains. The optical density of bacterial suspensions was monitored over time and compared to that of control strains *E. coli* CC118, which remained stable in suspension over time, and NTHi 375 Δ*hap*, a mutant displaying less self-aggregation than the wild-type strain (Table 3). NTHi 375 wild-type, Δ*siaB*, Δ*lic2A*, Δ*lgtF*, Δ*lpsA*, Δ*lgtF* Δ*lpsA*, and Δ*opsX* strains presented comparable aggregation profiles. NTHi 375 Δ*lic1* aggregated faster than the other strains, which reverted to wild-type levels with the complemented Δ*lic1ABCD*-c strain (Table 3; see also Fig. S3 in the supplemental material). These results suggest that under the conditions tested, PCho plays some role in NTHi self-aggregation.

Studies indicate that NTHi can form biofilm communities (4). We investigated the contribution of LOS epitopes to the formation of biofilm communities for NTHi 375 grown under continuous-flow culture conditions in microfermentors (50). We monitored biofilm development in microfermentors by measuring the turbidity of bacterial suspensions detached from removable glass slides (Fig. 2). Strains NTHi 375 Δ*lic1* and Δ*lgtF* ($P < 0.005$), as well as the Δ*siaB* and Δ*lgtF* Δ*lpsA* ($P < 0.0005$) mutants, were significantly impaired in biofilm formation compared to the wild-type strain. This deficiency was restored to a wild-type level for the complemented strains NTHi 375 Δ*lic1ABCD*-c and Δ*lgtF*-c. NTHi 375 Δ*lgtF* showed reduced biofilm formation, despite the presence of PCho and sialic acid in its LOS molecule, suggesting that the Glc on Hep I, or PCho linked to that residue, may play a prominent role in biofilm growth. NTHi 375 Δ*lgtF* Δ*lpsA* formed biofilms similar to those formed by the Δ*lgtF* single mutant. Strains NTHi 375 Δ*lic2A*, Δ*lpsA*, and Δ*opsX* formed biofilms not significantly different from those formed by the wild-type strain.

In sum, the results obtained show that PCho, sialic acid, and sugar extension on Hep I influence the capacity of NTHi to develop biofilm communities.

LOS sugar extension on Hep I is important to NTHi infection of epithelial cells, and the inner core modulates inflammation. The interplay of NTHi with the human respiratory epithelium plays a determinant role in the progression of the infection (51). We infected A549 cells, a model human type II pneumocyte cell line which NTHi 375 is known to adhere to and invade (41, 52), to assess the role of LOS in NTHi-host cell interplay. Adhesion of NTHi 375 Δ*lgtF*, Δ*lgtF*Δ*lpsA*, and Δ*opsX* was lower than that displayed by the wild-type strain (Fig. 3A). Following on from this observation, the same mutants invaded A549 cells significantly less than the wild-type strain. Complementation of the *lgtF* mutation restored invasion to wild-type levels (Fig. 3B). Intracellular bacteria were found to colocalize with a fluid marker of acidic subcellular compartments (Lysotracker) in all cases (data not shown), as shown before for the wild-type strain (41).

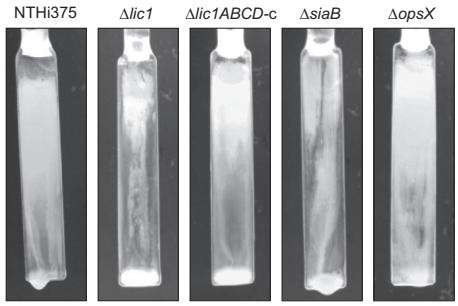

Strain	OD_{600nm} of bacterial suspension detached from glass slide
NTHi375	1.79±0.29
Δ*lic1*	0.99±0.48[a]
Δ*lic1ABCD*-c	1.58±0.07
Δ*siaB*	0.93±0.22[b]
Δ*lic2A*	1.48±0.14
Δ*lgtF*	0.91±0.45[a]
Δ*lgtF*-c	1.57±0.16
Δ*lpsA*	1.71±0.3
Δ*lgtF*Δ*lpsA*	1.08±0.35[b]
Δ*opsX*	1.83±0.11

FIG 2 Effect of LOS truncation on NTHi 375 biofilm formation under continuous-flow conditions, in microfermentors containing the glass slides where bacteria formed the biofilm. Images are from a representative experiment for wild-type NTHi 375 and Δ*lic1*, Δ*lic1ABCD*-c, Δ*siaB*, and Δ*opsX* mutants. The bottom panel shows the OD_{600} of bacterial suspension detached from glass slide for each strain. Data shown are means and SDs of absorbance values, compared by a two-tailed *t* test, versus those obtained for NTHi 375. [a] $P < 0.005$; [b] $P < 0.0005$.

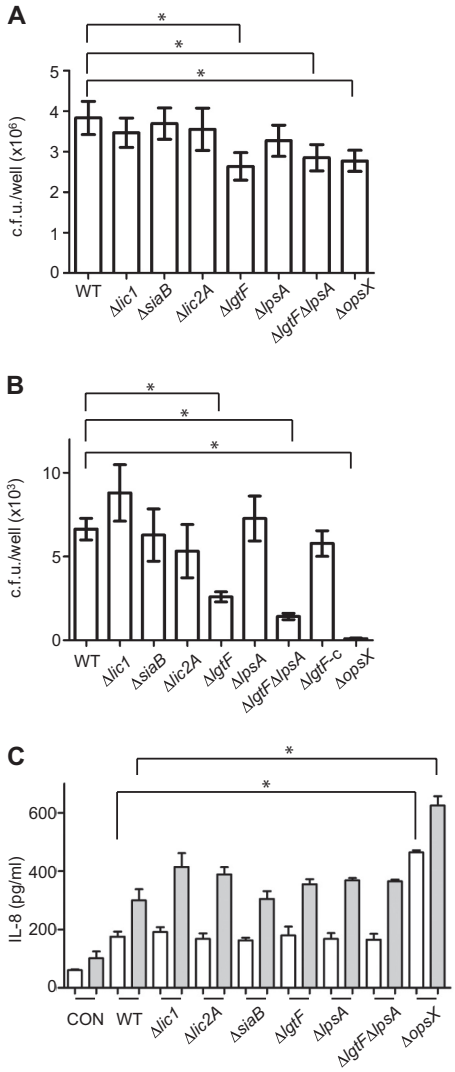

FIG 3 Infection of A549 epithelial cells by NTHi strains with serial LOS truncation. (A) Effect of LOS truncation on NTHi epithelial adhesion. Wild-type NTHi 375 and Δ*lic1*, Δ*siaB*, Δ*lic2A*, Δ*lgtF*, Δ*lpsA*, Δ*lgtF* Δ*lpsA*, and Δ*opsX* mutants were used to infect cells for 30 min. The number of bacteria adhered/well is shown for each strain. Mean numbers were significantly lower (*, $P < 0.05$) than those obtained for the wild-type strain for the Δ*lgtF*, Δ*lgtF* Δ*lpsA*, and Δ*opsX* mutants. (B) Effect of LOS truncation on NTHi epithelial cell invasion. Wild-type NTHi 375 and Δ*lic1*, Δ*siaB*, Δ*lic2A*, Δ*lgtF*, Δ*lgtF*-c, Δ*lpsA*, Δ*lgtF* Δ*lpsA*, and Δ*opsX* mutants were used to infect cells for 2 h. The number of invading bacteria/well is shown for each strain. Mean numbers were significantly lower (*, $P < 0.0001$) than those obtained for the wild-type strain for the Δ*lgtF*, Δ*lgtF* Δ*lpsA*, and Δ*opsX* mutants. (C) Effect of LOS truncation on NTHi-mediated inflammatory response. IL-8 secreted to the supernatant by cells upon infection with wild-type NTHi 375 and the Δ*lic1*, Δ*lic2A*, Δ*siaB*, Δ*lgtF*, Δ*lpsA*, Δ*lgtF* Δ*lpsA*, and Δ*opsX* mutants was quantified at 6 (white bars) and 20 (gray bars) h postinfection by ELISA. CON, noninfected cells. Mean numbers for the Δ*opsX* mutant were significantly (*, $P < 0.001$) higher than those obtained for the wild-type strain at 6 and 20 h postinfection.

We and others have shown previously that NTHi infection triggers the secretion of proinflammatory cytokines by epithelial cells (53). We sought to determine the impact of LOS structure on IL-8 secretion by A549 cells. Δ*lic1*, Δ*siaB*, Δ*lic2A*, Δ*lgtF*, Δ*lpsA*, and Δ*lgtF* Δ*lpsA* strains induced levels of IL-8 at 6 and 20 h postinfection similar to those induced by the wild-type strain. In contrast, infection with strain NTHi 375 Δ*opsX* stimulated the secretion of IL-8 to levels significantly higher than those triggered by the wild-type strain, at 6 and 20 h postinfection (Fig. 3C).

These data suggest that some LOS structure, such as the Hex on Hep I, may be important for NTHi infection of epithelial cells and that loss of all core structure impairs bacterial invasion and enhances the cell inflammatory response.

Contribution of LOS moieties to NTHi375 mouse pulmonary infection. NTHi persistence on a mouse infection model has been previously assessed by intratracheal or intranasal inoculation of pathogenic strains and mutant derivatives, or of mutant derivatives of the nonpathogenic strain *H. influenzae* Rd KW20 (25, 54–57). To assess the relative roles of LOS moieties in NTHi persistence and/or clearance within mice, we carried out intranasal infection of CD1 mice with NTHi 375 wild-type and mutant strains. NTHi 375 was used to establish infection dose, adequate intervals of study, and histopathological changes of respiratory tissues in the mouse model. Histopathological analysis of upper airways, trachea, and lungs from mice infected intranasally with NTHi 375 was performed by both H&E and IHC staining and compared with tissues from vehicle (PBS)-inoculated mice. The sections were examined blind as sets by a trained veterinary pathologist (M. Barberán). The microscopy score of the average lesion in samples of mice infected with NTHi 375 is shown in the bottom portion of Fig. 4. In the upper airways, the most severe lesions were observed at 24 h postinfection (p.i.), whereas in trachea and lungs, the lesions peaked at 48 h p.i. Lungs and airways from control mice instilled with PBS did not show either significant inflammation or pathological changes. By H&E, the upper airways showed some subepithelial and intravascular neutrophils and sloughed lining epithelial necrotic cells at 24 h p.i. (Fig. 4U1 and -U2). The lumens of the turbinates were filled with seropurulent exudate and detached epithelial cells. Immunostained NTHi antigen was located in the cytoplasm of some phagocytic cells present in the luminal exudate (Fig. 4U3). The most intense tracheal lesions were found in mice sacrificed at 48 h p.i., with a greater quantity of cellular exudate in the lumen (Fig. 4T1 and -T2). Immunostained NTHi antigen was located in phagocytic cells present in luminal exudates (Fig. 4T3). The most severe pulmonary histopathological lesions were also observed in mice euthanatized at 48 h p.i., showing large areas of acute bronchopneumonia (Fig. 4L1 and -L2). In these areas, alveolar septa were thickened and edematous and had an inflammatory infiltrate, mainly neutrophils and hyperplasic type 2 pneumonocytes. Alveolar spaces were filled with neutrophils, phagocytic mononucleated cells, and small alveolar hemorrhages. Suppurative bronchitis and bronchiolitis with neutrophilic subepithelial infiltrates and seropurulent exudates in the lumens were also observed. NTHi antigen was found in the cytoplasm of cells in the pneumonic areas (Fig. 4L3). These pathogenic findings in lungs correlated to bacterial loads of 5.13 ± 0.65 and 3.15 ± 0.48 log CFU/lung (means ± SDs) at 24 h and 48 h p.i., respectively (Fig. 5).

For the purpose of strain comparison, we quantified bacterial loads for each mutant from lung homogenates of infected mice at 24 and 48 h p.i. We recovered significantly fewer NTHi 375 Δ*lgtF* Δ*lpsA* (24 h p.i., $P < 0.05$; 48 h p.i., $P < 0.01$) and Δ*opsX* ($P < 0.001$) bacteria than bacteria of the parental strain at times (Fig. 5). NTHi 375 Δ*lgtF* rendered significantly fewer bacteria than the wild-type strain at 24 h p.i. ($P < 0.05$). NTHi 375 Δ*siaB* delivered counts indistinguishable from those obtained after infection with

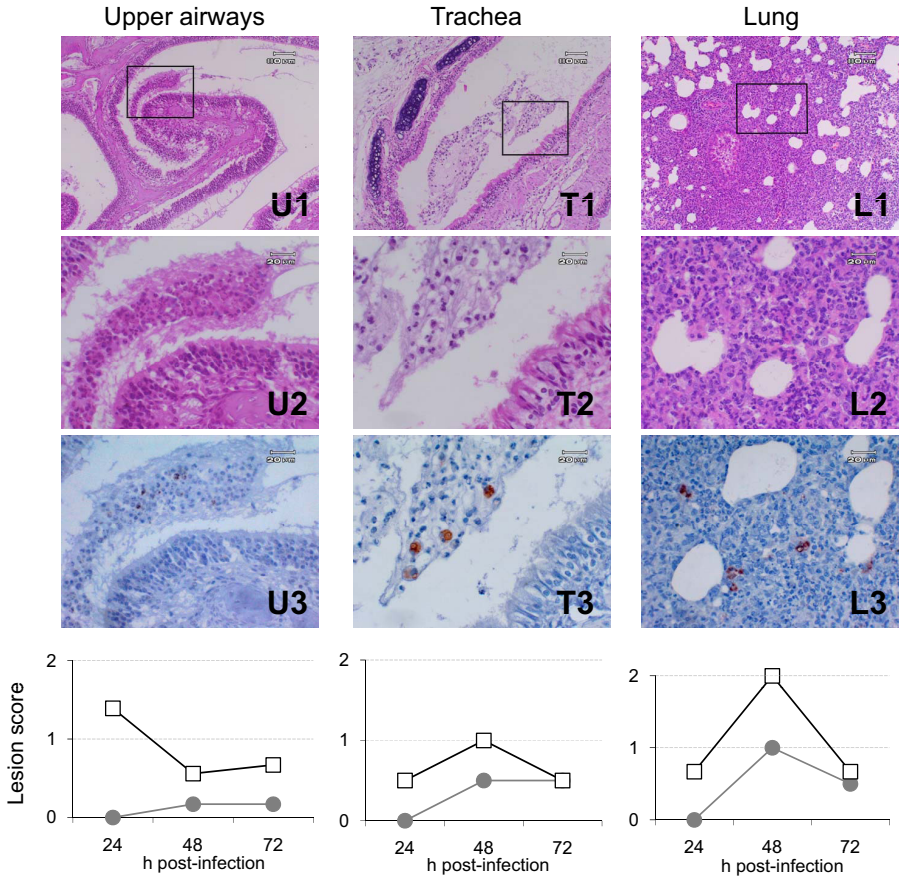

FIG 4 Histopathological findings and lesion scores in the respiratory system of CD1 mice intranasally infected with NTHi 375. (Top) Tissue sections were H&E stained and lesions subjectively scored on a scale from 0 to 3 (0, absent; 1, mild; 2, moderate; and 3, severe) for inflammatory markers. Selected tissue sections were also IHC stained to detect NTHi 375 antigen in the lesions. The left column shows upper airways from an infected mouse analyzed at 24 h p.i. (U1) Mild epithelial degeneration and necrosis and small amounts of luminal exudate (H&E). (U2) Detail of the lumen of the turbinate filled with serous exudate, neutrophils, and detached epithelial cells (H&E). (U3) NTHi antigen located in the cytoplasm of neutrophils in the luminal exudate (IHC). The middle column shows the trachea from an infected mouse sacrificed at 48 h p.i. (T1) Seropurulent exudate in the tracheal lumen (H&E). (T2) Detail of the exudate from T1 (H&E). (T3) Immunostained NTHi antigen located in the cytoplasm of large phagocytic cells present in the luminal exudate (IHC). The right column shows a lung from an infected mouse analyzed at 48 h p.i. (L1) Large areas of acute bronchopneumonia. (L2) Detail of alveolar spaces and thickened alveolar septa filled with neutrophils and macrophages. (L3) NTHi antigen in the cytoplasm of some phagocytic cells (IHC). (Bottom) Histopathological average lesion scores obtained from sections of upper airways (left), tracheas (middle), and lungs (right) at 24, 48, and 72 h p.i. In the upper airways, the most severe lesions were observed at 24 h p.i., whereas in trachea and lungs, the lesions peaked at 48 h p.i.

the wild-type strain. NTHi 375 Δ*lic1*, Δ*lic2A*, and Δ*lpsA* strains showed a slight but not significant reduction in the number of bacteria recovered, compared to the wild-type strain. Given that mutations causing the most severe LOS truncations caused a faster bacterial clearance from the lungs of infected mice than that shown by the wild-type strain, data indicate that LOS decoration is likely to delay the clearance of NTHi in mice pulmonary infections.

DISCUSSION

This study delineates novel roles for LOS moieties in a number of properties related to the pathogenesis of NTHi. Our in-depth comparison of serially truncated LOS in mutants in a strain background whose LOS structure had been previously determined has systematically established for the first time correlations between specific LOS moieties and a range of characteristics underlying pathogenic traits. Previous studies have explored LOS phenotypes in groups of NTHi mutants. The abilities of NTHi 2019 Δ*siaB*, Δ*siaA*, and Δ*lsgB* mutants to form biofilms have been compared *in vitro* (28) and *in vivo* (29); the persistence of NTHi 2019 Δ*licD* and Δ*siaB* mutants in mouse lungs has been assessed (25, 56), and the interference of LOS biosynthetic gene inactivation on Hap outer membrane location has been tested in *H. influenzae* Rd KW20 (58). Also, high-throughput insertion tracking by deep sequencing (HITS) showed the importance of LOS structure for *H. influenzae* Rd KW20 survival in the mouse lung (54). None of these studies utilized mutant strain panels expressing serial LOS truncation in a pathogenic strain background. In this study, we used NTHi 375, an isolate that naturally lacks any sugar extension on Hep II given that it lacks the *lic2C* gene, focusing the study on sugar extensions on Hep I and III (Fig. 1A). The frequency of *lic2C* distribution among strains is variable, depending on the strain set (8, 59). We generated a series of mutants that express serial LOS truncations and then assessed their effect on a number of traits relating to bacterial interplay with the host. A summary of the results obtained is shown in Fig. 6. Our results indicate that PCho

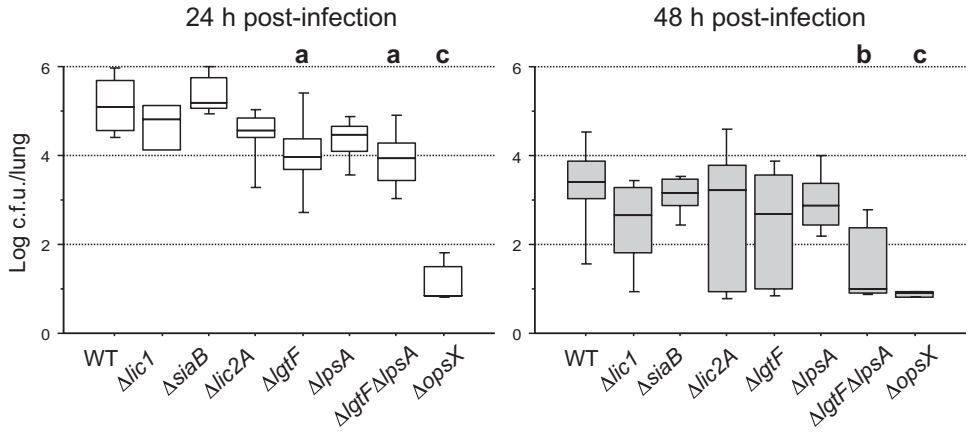

FIG 5 Bacterial loads in the lungs of CD1 mice infected by NTHi strains with serial LOS truncation. Mice were infected intranasally with ~10^8 bacteria. Bacterial counts in lungs at 24 or 48 h p.i. were determined. Results are reported as $\log_{10}$ CFU/lung and represented as box plot graphs (lines inside boxes represent median values). Statistical differences versus the wild-type strain are indicated as follows: a, $P < 0.05$; b, $P < 0.01$; and c, $P < 0.001$.

not only is important for protecting NTHi against LL-37/hCAP18 (20) but also protects from PxB and hBD-1 and supports its role in biofilm formation (21, 23, 25, 60). NTHi 375 Δ*lic1* was the only mutant tested presenting a significant increase in self-aggregation, maybe related to the favored exposure of molecules important for this bacterial property. NTHi 375 displays PCho on a Glc on Hep I; given that NTHi 375 Δ*lgtF*, lacking such a Glc on Hep I, rendered a positive signal for PCho, this modification is likely to locate on Hep III in this mutant. Therefore, we speculate that properties displayed by NTHi 375 Δ*lgtF* could relate to the absence of a sugar extension on Hep I and/or the presence of PCho on a Hex on Hep III, which could be due to some activity for Lic1D, allowing it to have some dual functionality depending upon the array of glycoforms presented as the template during LPS synthesis. In any case, we demonstrate a previously unknown involvement of Glc on Hep I in bacterial resistance to PxB and hBD-1, in biofilm growth, and in epithelial infection. Intratracheal injection of NTHi 2019 and 86-028NP wild-type and *licD* mutant derivatives into mice showed that this mutant exhibited a modest strain-specific attenuation at 24 h p.i., more consistent at 48 h p.i. (25, 61). Separately, intranasal infection of mice with an *H. influenzae* Rd KW20 transposon insertion mutant library showed that the *lic1D* gene was nonessential in the lungs (54). In that study, the mouse pulmonary infection model used rendered a mild, nonsignificant involvement of PCho in bacterial persistence in the lung. Conversely, NTHi 375 Δ*lgtF* clearance from lung homogenates was higher than that of the wild-type strain, mainly at 24 h p.i. A minor role for *lgtF* in NTHi survival in the lung has been

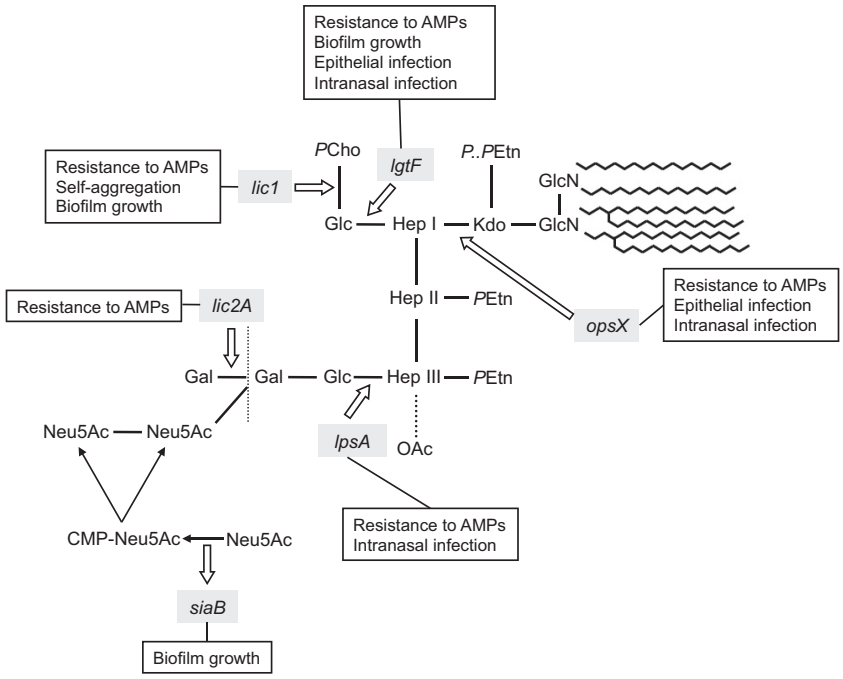

FIG 6 Summary of the specific contributions of NTHi LOS inner and outer core moieties to virulence properties delineated in this study.

suggested by HITS (54), and this is the first time a defined NTHi Δ*lgtF* mutant has been tested *in vivo*.

The digalactose moiety confers resistance to serum killing (17). In this study, it also appears to play some role in resistance to killing by AMPs. Conversely, sialic acid, known to play a role in bacterial resistance to serum (14), did not seem to influence NTHi resistance to AMPs. Our data confirmed the previously identified role of sialic acid in biofilm growth (28–30). Moreover, NTHi 375 Δ*lic2A* and Δ*siaB* mutants did not display significant defects in bacterial persistence in the mouse lung. A role for sialic acid in NTHi survival in the lung had been previously excluded by mice intratracheal injection of NTHi 2019 wild-type and *siaB* mutant strains (56). However, Neu5Ac substitution of LOS seems to play a key role in experimental OM (31). Strain NTHi 375 Δ*siaB* retains the ability to take up sialic acid from the host (a functional sialic acid uptake system is conserved) but cannot activate the sugar, thereby abrogating all Neu5Ac incorporation into LOS glycoforms.

We also show a further phenotype for sugar extension on Hep III of LOS, previously involved in NTHi resistance to serum killing (8). NTHi 375 Δ*lpsA* was less resistant to killing by AMPs PxB and hBD-1, indicating a role for the sugar extension on Hep III, which includes the digalactose, in this process. Interestingly, NTHi 375 Δ*lpsA* formed a biofilm indistinguishable from that of the wild-type strain, an unexpected result given that this mutant lacks sialic acid. We speculate that truncation of the sugar extension on Hep III allows other structures in the LOS important for biofilm growth to be more prominently exposed, compensating for the absence of sialic acid. Of note, it has been reported that NTHi 2019 Δ*pgmB*, a mutant expressing LOS truncated at the triheptose core, forms a biofilm (28). Simultaneous mutation of *lgtF* and *lpsA* in NTHi 375 suggests a synergy for extensions on Hep I and III on bacterial resistance to AMPs and on survival in the lung. Biofilm growth and NTHi interaction with epithelial cells were similar for NTHi 375 Δ*lgtF* Δ*lpsA* and Δ*lgtF* strains, suggesting a dominant effect of sugar extension on Hep I on those virulence traits.

The most truncated mutant, NTHi 375 Δ*opsX*, lacking all core sugars and exposing the Kdo attached to lipid A, showed a significant defect in bacterial resistance to AMPs. Serial LOS truncation may alter the hydrophobic properties of the bacterial cell surface, such that removal of particular epitopes, or combinations of them, may result in a significantly more hydrophobic surface environment. As reported for other pathogens, a stepwise elevation in the surface hydrophobicity on shorter LOS chains could make the microbe more susceptible to AMPs (62). The Δ*opsX* mutation also restricted bacterial epithelial invasion, but it still enabled a robust biofilm to be formed. LPSs from other bacteria have also been shown to influence biofilm production. For example, the absence of the outer core on *Campylobacter jejuni* LOS enhances biofilm formation (63). These data support a model in which the cell envelope is dynamic, with compensatory changes in response to truncation or elimination of others, likely selected for under certain cultural and environmental conditions. Indeed, LOS expression seems to be altered during NTHi growth as a biofilm compared to planktonic growth (64), evidence obtained through reactivity of the LPS monoclonal antibody (MAb) 6E4, which binds to an inner core LPS epitope that includes the Kdo structure (65). Given that NTHi 375 Δ*opsX* formed a robust biofilm, and that MAb 6E4 rendered a significant signal on biofilm grown bacterial extracts (64), data support a positive role for Kdo on the NTHi biofilm interface. NTHi 375 Δ*opsX* also induced an enhanced proinflammatory response upon epithelial cell infection. O antigen has been proposed to mediate evasion from early epithelial innate immune activation by delaying LPS recognition for other pathogens (66). NTHi 375 Δ*opsX* was severely attenuated for infecting the lung, in agreement with HITS data (54). We speculate that this impairment could be related to enhanced susceptibilities to AMPs and serum, together with stimulation of an effective proinflammatory response.

The phase variation of LOS epitopes exerted through nucleotide repeats situated within biosynthetic genes is important for *H. influenzae*-host interplay and pathogenesis. For example, the dynamics of *H. influenzae* LOS expression following exposure to human serum have been recently examined by sequencing the 5′ end of LOS-related phase-variable genes from bacteria that have evaded complement-mediated killing. This revealed a shift from a phase-off to a phase-on status in several phase-variable genes, and incorporation of the respective epitopes into LOS could account for the observed evasion of complement (67). In this study, we have systematically assessed a range of virulence related phenotypes in mutant strains expressing serially truncated LOS, with an aim to establish gene-to-function relationships. Most of these mutants express LOS of reduced complexity and correspondingly incorporate fewer phase-variable epitopes compared to those of the wild-type strain. However, some potential effect of phase variation of LOS epitopes on those phenotypes cannot be excluded and would be of interest to investigate in future studies.

The phenotypic screening performed also allowed framing of these traits in the context of infection. The most truncated mutants, NTHi 375 Δ*opsX* and Δ*lgtF* Δ*lpsA*, displayed a significant impairment in their ability to interact with AMPs and epithelial cells and to infect mice. Conversely, these mutants did not display differences in self-aggregation, compared to the wild-type strain, and the former strain formed a robust biofilm. NTHi 375 Δ*lic1* and Δ*lic2A* displayed an increased sensitivity to AMPs, and NTHi 375 Δ*lic1* and Δ*siaB* displayed an impaired ability to form biofilm; however, these mutants did not show significant defects in lung survival. The results obtained for NTHi 375 Δ*lgtF*, Δ*lpsA*, and Δ*lgtF* Δ*lpsA* suggest that Glc extension on Hep I and III may have additive effects on bacterial resistance to AMPs but that extension on Hep I may have a dominant role on bacterial biofilm growth and epithelial interplay. Regarding lung infection, the reduced initial infection of NTHi 375 Δ*lgtF* Δ*lpsA* could be attributable to a defect in the Hep I branch (i.e., Δ*lgtF*), even though data obtained at 48 h p.i. suggest that sugar extensions from Hep I and III may play nonredundant roles on NTHi lung survival. Altogether, this study further reinforces the importance of LOS molecule on NTHi pathogenicity, uncovers novel gene-function associations for LOS moieties, and supports the notion that NTHi-host interplay is a complex multifactorial process influenced by numerous features of both the bacterium and the host.

ACKNOWLEDGMENTS

We appreciate technical support by and helpful discussions with J. Moleres, S. Mauro and I. Moriyón, I. Lasa, E. Llobet, P. Martí-Lliteras, and A. López-Gómez.

This work has been funded by grants from Instituto de Salud Carlos III, reference numbers CP05/00027, PI06/1251, and PS09/00130, and from MINECO SAF2012-31166 to J.G. CIBERES is an initiative from Instituto de Salud Carlos III, Spain.

REFERENCES

1. **Agrawal A, Murphy TF.** 2011. *Haemophilus influenzae* infections in the *H. influenzae* type b conjugate vaccine era. J. Clin. Microbiol. **49:**3728–3732.
2. **Apicella MA.** 2012. Nontypeable *Haemophilus influenzae*: the role of N-acetyl-5-neuraminic acid in biology. Front. Cell. Infect. Microbiol. **2:**19. doi:10.3389/fcimb.2012.00019.
3. **Hallström T, Riesbeck K.** 2010. *Haemophilus influenzae* and the complement system. Trends Microbiol. **18:**258–265.
4. **Swords WE.** 2012. Nontypeable *Haemophilus influenzae* biofilms: role in chronic airway infections. Front. Cell. Infect. Microbiol. **2:**97. doi:10.3389/fcimb.2012.00097.
5. **Schweda EK, Richards JC, Hood DW, Moxon ER.** 2007. Expression and structural diversity of the lipopolysaccharide of *Haemophilus influenzae*: implication in virulence. Int. J. Med. Microbiol. **297:**297–306.
6. **Gronow S, Brabetz W, Lindner B, Brade H.** 2005. OpsX from *Haemophilus influenzae* represents a novel type of heptosyltransferase I in lipopolysaccharide biosynthesis. J. Bacteriol. **187:**6242–6247.
7. **Deadman ME, Lundstrom SL, Schweda EK, Moxon ER, Hood DW.** 2006. Specific amino acids of the glycosyltransferase LpsA direct the addition of glucose or galactose to the terminal inner core heptose of *Haemophilus influenzae* lipopolysaccharide via alternative linkages. J. Biol. Chem. **281:**29455–29467.
8. **Hood DW, Deadman ME, Cox AD, Makepeace K, Martin A, Richards JC, Moxon ER.** 2004. Three genes, *lgtF, lic2C* and *lpsA*, have a primary role in determining the pattern of oligosaccharide extension from the inner core of *Haemophilus influenzae* LPS. Microbiology **150:**2089–2097.
9. **Mansson M, Bauer SH, Hood DW, Richards JC, Moxon ER, Schweda EK.** 2001. A new structural type for *Haemophilus influenzae* lipopolysaccharide. Structural analysis of the lipopolysaccharide from nontypeable *Haemophilus influenzae* strain 486. Eur. J. Biochem. **268:**2148–2159.
10. **Weiser JN, Shchepetov M, Chong ST.** 1997. Decoration of lipopolysaccharide with phosphorylcholine: a phase-variable characteristic of *Haemophilus influenzae*. Infect. Immun. **65:**943–950.
11. **High NJ, Deadman ME, Moxon ER.** 1993. The role of a repetitive DNA motif (5′-CAAT-3′) in the variable expression of the *Haemophilus influenzae* lipopolysaccharide epitope α Gal(1–4)β Gal. Mol. Microbiol. **9:**1275–1282.
12. **Fox KL, Cox AD, Gilbert M, Wakarchuk WW, Li J, Makepeace K, Richards JC, Moxon ER, Hood DW.** 2006. Identification of a bifunctional lipopolysaccharide sialyltransferase in *Haemophilus influenzae*: incorporation of disialic acid. J. Biol. Chem. **281:**40024–40032.
13. **Hood DW, Cox AD, Gilbert M, Makepeace K, Walsh S, Deadman ME, Cody A, Martin A, Mansson M, Schweda EK, Brisson JR, Richards JC, Moxon ER, Wakarchuk WW.** 2001. Identification of a lipopolysaccharide α-2,3-sialyltransferase from *Haemophilus influenzae*. Mol. Microbiol. **39:**341–350.
14. **Hood DW, Makepeace K, Deadman ME, Rest RF, Thibault P, Martin A, Richards JC, Moxon ER.** 1999. Sialic acid in the lipopolysaccharide of *Haemophilus influenzae*: strain distribution, influence on serum resistance and structural characterization. Mol. Microbiol. **33:**679–692.
15. **Jones PA, Samuels NM, Phillips NJ, Munson RS, Jr, Bozue JA, Arseneau JA, Nichols WA, Zaleski A, Gibson BW, Apicella MA.** 2002. *Haemophilus influenzae* type b strain A2 has multiple sialyltransferases involved in lipooligosaccharide sialylation. J. Biol. Chem. **277:**14598–14611.
16. **Lysenko E, Richards JC, Cox AD, Stewart A, Martin A, Kapoor M, Weiser JN.** 2000. The position of phosphorylcholine on the lipopolysaccharide of *Haemophilus influenzae* affects binding and sensitivity to C-reactive protein-mediated killing. Mol. Microbiol. **35:**234–245.
17. **Weiser JN, Pan N.** 1998. Adaptation of *Haemophilus influenzae* to acquired and innate humoral immunity based on phase variation of lipopolysaccharide. Mol. Microbiol. **30:**767–775.
18. **Weiser JN, Pan N, McGowan KL, Musher D, Martin A, Richards J.** 1998. Phosphorylcholine on the lipopolysaccharide of *Haemophilus influenzae* contributes to persistence in the respiratory tract and sensitivity to serum killing mediated by C-reactive protein. J. Exp. Med. **187:**631–640.
19. **Clark SE, Snow J, Li J, Zola TA, Weiser JN.** 2012. Phosphorylcholine allows for evasion of bactericidal antibody by *Haemophilus influenzae*. PLoS Pathog. **8:**e1002521. doi:10.1371/journal.ppat.1002521.
20. **Lysenko ES, Gould J, Bals R, Wilson JM, Weiser JN.** 2000. Bacterial phosphorylcholine decreases susceptibility to the antimicrobial peptide LL-37/hCAP18 expressed in the upper respiratory tract. Infect. Immun. **68:**1664–1671.
21. **Hong W, Mason K, Jurcisek J, Novotny L, Bakaletz LO, Swords WE.** 2007. Phosphorylcholine decreases early inflammation and promotes the establishment of stable biofilm communities of nontypeable *Haemophilus influenzae* strain 86-028NP in a chinchilla model of otitis media. Infect. Immun. **75:**958–965.
22. **Hong W, Pang B, West-Barnette S, Swords WE.** 2007. Phosphorylcholine expression by nontypeable *Haemophilus influenzae* correlates with maturation of biofilm communities *in vitro* and *in vivo*. J. Bacteriol. **189:**8300–8307.
23. **West-Barnette S, Rockel A, Swords WE.** 2006. Biofilm growth increases phosphorylcholine content and decreases potency of nontypeable *Haemophilus influenzae* endotoxins. Infect. Immun. **74:**1828–1836.
24. **Swords WE, Ketterer MR, Shao J, Campbell CA, Weiser JN, Apicella MA.** 2001. Binding of the non-typeable *Haemophilus influenzae* lipooligosaccharide to the PAF receptor initiates host cell signalling. Cell. Microbiol. **3:**525–536.
25. **Pang B, Winn D, Johnson R, Hong W, West-Barnette S, Kock N, Swords WE.** 2008. Lipooligosaccharides containing phosphorylcholine delay pulmonary clearance of nontypeable *Haemophilus influenzae*. Infect. Immun. **76:**2037–2043.
26. **Griffin R, Bayliss CD, Herbert MA, Cox AD, Makepeace K, Richards JC, Hood DW, Moxon ER.** 2005. Digalactoside expression in the lipopolysaccharide of *Haemophilus influenzae* and its role in intravascular survival. Infect. Immun. **73:**7022–7026.
27. **Figueira MA, Ram S, Goldstein R, Hood DW, Moxon ER, Pelton SI.** 2007. Role of complement in defense of the middle ear revealed by restoring the virulence of nontypeable *Haemophilus influenzae siaB* mutants. Infect. Immun. **75:**325–333.
28. **Greiner LL, Watanabe H, Phillips NJ, Shao J, Morgan A, Zaleski A, Gibson BW, Apicella MA.** 2004. Nontypeable *Haemophilus influenzae* strain 2019 produces a biofilm containing N-acetylneuraminic acid that may mimic sialylated O-linked glycans. Infect. Immun. **72:**4249–4260.
29. **Jurcisek J, Greiner L, Watanabe H, Zaleski A, Apicella MA, Bakaletz LO.** 2005. Role of sialic acid and complex carbohydrate biosynthesis in biofilm formation by nontypeable *Haemophilus influenzae* in the chinchilla middle ear. Infect. Immun. **73:**3210–3218.
30. **Swords WE, Moore ML, Godzicki L, Bukofzer G, Mitten MJ, VonCannon J.** 2004. Sialylation of lipooligosaccharides promotes biofilm formation by nontypeable *Haemophilus influenzae*. Infect. Immun. **72:**106–113.
31. **Bouchet V, Hood DW, Li J, Brisson JR, Randle GA, Martin A, Li Z, Goldstein R, Schweda EK, Pelton SI, Richards JC, Moxon ER.** 2003. Host-derived sialic acid is incorporated into *Haemophilus influenzae* lipopolysaccharide and is a major virulence factor in experimental otitis media. Proc. Natl. Acad. Sci. U. S. A. **100:**8898–8903.
32. **Martí-Lliteras P, Regueiro V, Morey P, Hood DW, Saus C, Sauleda J, Agusti AG, Bengoechea JA, Garmendia J.** 2009. Nontypeable *Haemophilus influenzae* clearance by alveolar macrophages is impaired by exposure to cigarette smoke. Infect. Immun. **77:**4232–4242.
33. **Fleischmann RD, Adams MD, White O, Clayton RA, Kirkness EF, Kerlavage AR, Bult CJ, Tomb JF, Dougherty BA, Merrick JM, et al.** 1995. Whole-genome random sequencing and assembly of *Haemophilus influenzae* Rd. Science **269:**496–512.
34. **Harrison A, Dyer DW, Gillaspy A, Ray WC, Mungur R, Carson MB, Zhong H, Gipson J, Gipson M, Johnson LS, Lewis L, Bakaletz LO, Munson RS, Jr.** 2005. Genomic sequence of an otitis media isolate of nontypeable *Haemophilus influenzae*: comparative study with *H. influenzae* serotype d, strain KW20. J. Bacteriol. **187:**4627–4636.
35. **Allen S, Zaleski A, Johnston JW, Gibson BW, Apicella MA.** 2005. Novel sialic acid transporter of *Haemophilus influenzae*. Infect. Immun. **73:**5291–5300.
36. **Herriott RM, Meyer EY, Vogt M, Modan M.** 1970. Defined medium for growth of *Haemophilus influenzae*. J. Bacteriol. **101:**513–516.
37. **Johnston JW, Zaleski A, Allen S, Mootz JM, Armbruster D, Gibson BW, Apicella MA, Munson RS, Jr.** 2007. Regulation of sialic acid transport and catabolism in *Haemophilus influenzae*. Mol. Microbiol. **66:**26–39.
38. **Lesse AJ, Campagnari AA, Bittner WE, Apicella MA.** 1990. Increased resolution of lipopolysaccharides and lipooligosaccharides utilizing tricine-sodium dodecyl sulfate-polyacrylamide gel electrophoresis. J. Immunol. Methods **126:**109–117.
39. **Swords WE, Buscher BA, Ver Steeg Ii K, Preston A, Nichols WA, Weiser JN, Gibson BW, Apicella MA.** 2000. Non-typeable *Haemophilus*

influenzae adhere to and invade human bronchial epithelial cells via an interaction of lipooligosaccharide with the PAF receptor. Mol. Microbiol. **37:**13–27.
40. **Llobet E, Campos MA, Gimenez P, Moranta D, Bengoechea JA.** 2011. Analysis of the networks controlling the antimicrobial-peptide-dependent induction of *Klebsiella pneumoniae* virulence factors. Infect. Immun. **79:**3718–3732.
41. **Morey P, Cano V, Marti-Lliteras P, Lopez-Gomez A, Regueiro V, Saus C, Bengoechea JA, Garmendia J.** 2011. Evidence for a non-replicative intracellular stage of nontypable *Haemophilus influenzae* in epithelial cells. Microbiology **157:**234–250.
42. **Brogden KA.** 2005. Antimicrobial peptides: pore formers or metabolic inhibitors in bacteria? Nat. Rev. Microbiol. **3:**238–250.
43. **Hancock RE, Chapple DS.** 1999. Peptide antibiotics. Antimicrob. Agents Chemother. **43:**1317–1323.
44. **Nicolas P, Mor A.** 1995. Peptides as weapons against microorganisms in the chemical defense system of vertebrates. Annu. Rev. Microbiol. **49:**277–304.
45. **Vaara M.** 1992. Agents that increase the permeability of the outer membrane. Microbiol. Rev. **56:**395–411.
46. **Evans ME, Feola DJ, Rapp RP.** 1999. Polymyxin B sulfate and colistin: old antibiotics for emerging multiresistant gram-negative bacteria. Ann. Pharmacother. **33:**960–967.
47. **Hermsen ED, Sullivan CJ, Rotschafer JC.** 2003. Polymyxins: pharmacology, pharmacokinetics, pharmacodynamics, and clinical applications. Infect. Dis. Clin. North Am. **17:**545–562.
48. **Agerberth B, Grunewald J, Castanos-Velez E, Olsson B, Jornvall H, Wigzell H, Eklund A, Gudmundsson GH.** 1999. Antibacterial components in bronchoalveolar lavage fluid from healthy individuals and sarcoidosis patients. Am. J. Respir. Crit. Care Med. **160:**283–290.
49. **Hendrixson DR, St Geme JW, III.** 1998. The *Haemophilus influenzae* Hap serine protease promotes adherence and microcolony formation, potentiated by a soluble host protein. Mol. Cell **2:**841–850.
50. **Vergara-Irigaray M, Valle J, Merino N, Latasa C, Garcia B, Ruiz de Los Mozos I, Solano C, Toledo-Arana A, Penades JR, Lasa I.** 2009. Relevant role of fibronectin-binding proteins in *Staphylococcus aureus* biofilm-associated foreign-body infections. Infect. Immun. **77:**3978–3991.
51. **Clementi CF, Murphy TF.** 2011. Non-typeable *Haemophilus influenzae* invasion and persistence in the human respiratory tract. Front. Cell. Infect. Microbiol. **1:**1. doi:10.3389/fcimb.2011.00001.
52. **López-Gómez A, Cano V, Moranta D, Morey P, Garcia del Portillo F, Bengoechea JA, Garmendia J.** 2012. Host cell kinases, α5 and β1 integrins, and Rac1 signalling on the microtubule cytoskeleton are important for non-typable *Haemophilus influenzae* invasion of respiratory epithelial cells. Microbiology **158:**2384–2398.
53. **Regueiro V, Campos MA, Morey P, Sauleda J, Agusti AG, Garmendia J, Bengoechea JA.** 2009. Lipopolysaccharide-binding protein and CD14 are increased in the bronchoalveolar lavage fluid of smokers. Eur. Respir. J. **33:**273–281.
54. **Gawronski JD, Wong SM, Giannoukos G, Ward DV, Akerley BJ.** 2009. Tracking insertion mutants within libraries by deep sequencing and a genome-wide screen for *Haemophilus* genes required in the lung. Proc. Natl. Acad. Sci. U. S. A. **106:**16422–16427.
55. **Pang B, Hong W, Kock ND, Swords WE.** 2012. Dps promotes survival of nontypeable *Haemophilus influenzae* in biofilm communities *in vitro* and resistance to clearance *in vivo*. Front. Cell. Infect. Microbiol. **2:**58. doi:10.3389/fcimb.2012.00058.
56. **Pang B, Hong W, West-Barnette SL, Kock ND, Swords WE.** 2008. Diminished ICAM-1 expression and impaired pulmonary clearance of nontypeable *Haemophilus influenzae* in a mouse model of chronic obstructive pulmonary disease/emphysema. Infect. Immun. **76:**4959–4967.
57. **Rosadini CV, Gawronski JD, Raimunda D, Arguello JM, Akerley BJ.** 2011. A novel zinc binding system, ZevAB, is critical for survival of nontypeable *Haemophilus influenzae* in a murine lung infection model. Infect. Immun. **79:**3366–3376.
58. **Spahich NA, Hood DW, Moxon ER, St Geme JW, III.** 2012. Inactivation of *Haemophilus influenzae* lipopolysaccharide biosynthesis genes interferes with outer membrane localization of the hap autotransporter. J. Bacteriol. **194:**1815–1822.
59. **Martí-Lliteras P, Lopez-Gomez A, Mauro S, Hood DW, Viadas C, Calatayud L, Morey P, Servin A, Linares J, Oliver A, Bengoechea JA, Garmendia J.** 2011. Nontypable *Haemophilus influenzae* displays a prevalent surface structure molecular pattern in clinical isolates. PLoS One **6:**e21133. doi:10.1371/journal.pone.0021133.
60. **Hogg JS, Hu FZ, Janto B, Boissy R, Hayes J, Keefe R, Post JC, Ehrlich GD.** 2007. Characterization and modeling of the *Haemophilus influenzae* core and supragenomes based on the complete genomic sequences of Rd and 12 clinical nontypeable strains. Genome Biol. **8:**R103. doi:10.1186/gb-2007-8-6-r103.
61. **Wong SM, Akerley BJ.** 2012. Genome-scale approaches to identify genes essential for *Haemophilus influenzae* pathogenesis. Front. Cell. Infect. Microbiol. **2:**23. doi:10.3389/fcimb.2012.00023.
62. **Iwata T, Chiku K, Amano K, Kusumoto M, Ohnishi-Kameyama M, Ono H, Akiba M.** 2013. Effects of lipooligosaccharide inner core truncation on bile resistance and chick colonization by *Campylobacter jejuni*. PLoS One **8:**e56900. doi:10.1371/journal.pone.0056900.
63. **Naito M, Frirdich E, Fields JA, Pryjma M, Li J, Cameron A, Gilbert M, Thompson SA, Gaynor EC.** 2010. Effects of sequential *Campylobacter jejuni* 81-176 lipooligosaccharide core truncations on biofilm formation, stress survival, and pathogenesis. J. Bacteriol. **192:**2182–2192.
64. **Murphy TF, Kirkham C.** 2002. Biofilm formation by nontypeable *Haemophilus influenzae*: strain variability, outer membrane antigen expression and role of pili. BMC Microbiol. **2:**7. doi:10.1186/1471-2180-2-7.
65. **McLaughlin R, Spinola SM, Apicella MA.** 1992. Generation of lipooligosaccharide mutants of *Haemophilus influenzae* type b. J. Bacteriol. **174:**6455–6459.
66. **Duerr CU, Zenk SF, Chassin C, Pott J, Gutle D, Hensel M, Hornef MW.** 2009. O-antigen delays lipopolysaccharide recognition and impairs antibacterial host defense in murine intestinal epithelial cells. PLoS Pathog. **5:**e1000567. doi:10.1371/journal.ppat.1000567.
67. **Clark SE, Eichelberger KR, Weiser JN.** 2013. Evasion of killing by human antibody and complement through multiple variations in the surface oligosaccharide of *Haemophilus influenzae*. Mol. Microbiol. **88:**603–618.